Comparison of the single-proton pickup reactions ^{40}Ca(^{11}B,^{12}C)^{39}K and ^{40}Ca(^{13}C,^{14}N)^{39}K at low and high bombarding energies

C. F. Maguire, G. L. Bomar, A. V. Ramayya, and R. B. Piercey

Physics Department, Vanderbilt University, Nashville, Tennessee 37235

J. L. C. Ford, Jr., J. Gomez del Campo, D. Shapira, and D. Hensley

Oak Ridge National Laboratory, Oak Ridge, Tennessee 37830

(Received 26 December 1979; revised manuscript received 23 April 1980)

The single-proton pickup reactions ^{40}Ca(^{11}B,^{12}C)^{39}K and ^{40}Ca(^{13}C,^{14}N)^{39}K are found to produce qualitatively different angular distributions when compared at similar bombarding energies. The surface transparent potential invoked to explain the forward rise in the ^{40}Ca(^{13}C,^{14}N)^{39}K differential cross section at 40 MeV is shown to be inappropriate for the ^{40}Ca(^{11}B,^{12}C)^{39}K data analysis at 32 MeV incident energy. For the higher energy measurements at 68 MeV, both systems produce oscillatory angular distributions, but in the former case the distorted-wave Born approximation prediction is out of phase with the data, while in the latter it is exactly in phase with the data. The success of the distorted-wave Born approximation in predicting the magnitude of the cross sections is also different in the two cases.

NUCLEAR REACTIONS ^{40}Ca(^{11}B,^{12}C), $E=32$ and 68 MeV; ^{40}Ca(^{13}C,^{14}N), $E=40$ and 68 MeV; DWBA analysis of reactions; optical potential derived for elastic scattering.

I. INTRODUCTION

Recent studies[1,2] of the ^{40}Ca(^{13}C,^{14}N)^{39}K (g.s., 2.53 MeV $Q_0 = -0.779$) reactions at incident energies of 40, 60, and 68 MeV have yielded experimental angular distributions which could not be readily reproduced by standard distorted-wave Born-approximation (DWBA) calculations. At 40 MeV, as shown in Fig. 1, the large forward angle enhancement of the ground state differential cross section is absent from the shape predicted using a conventional volume absorption parametrization of the optical potential. By introducing a shallow surface absorption term effective outside a reduced region of strong volume absorption, Baltz *et al.*,[1] were able to obtain a theoretical curve in good agreement with their data. However, later measurements at higher energies[2] revealed that the surface-transparent description was no longer helpful, and in fact, the oscillatory behavior of the experimental angular distributions was almost exactly out of phase with the predicted shapes calculated from conventional optical potentials. That is, these data were part of the class of "$l=1$ anomalous" angular distributions.[3-5]

In order to determine the generality of the surface-transparent concept, and also to determine if the anomalous phasing persists in a more kinematically favored reaction we have studied the ^{40}Ca(^{11}B,^{12}C)^{39}K (g.s., $\frac{3}{2}^+$; 2.53 MeV, $\frac{1}{2}^+$; $Q_0 = +7.628$ MeV) reactions at 32 MeV and at 68 MeV incident energies. At the lower energy, this system is at nearly the same fractional height above the barrier

as the 40 MeV ^{40}Ca(^{13}C, ^{14}N)^{39}K experiment, while at the higher energy the present reaction is much closer to the optimum Q value. The Q-value difference between the two reactions affects not only the distorted waves in a DWBA calculation, but since it represents a tighter binding of the transferred nucleon in the ejectile in the (^{11}B, ^{12}C) reaction, the ^{40}Ca(^{11}B, ^{12}C)^{39}K study is also sensitive to a more interior region of the form factor than in the case of the ^{40}Ca(^{13}C, ^{14}N) reaction.
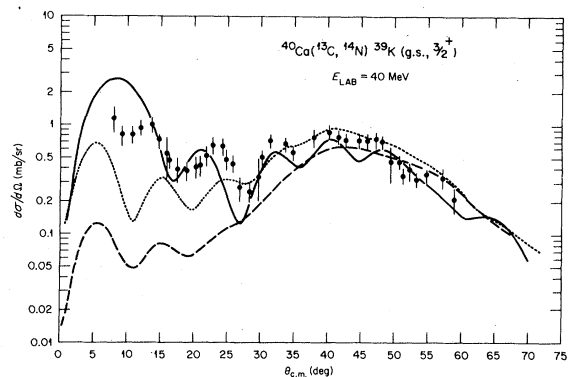

FIG. 1. Angular distribution of the ^{40}Ca(^{13}C,^{14}N)^{39}K (g.s.) reaction at 40 MeV incident energy (Ref. 1). The dashed curve is the exact-finite-range (EFR) prediction using the optical potential set 2($V=33.4$ MeV, $W=18$ MeV, $r_{R,I}=1.27$ fm, $a_{R,I}=0.55$ fm) of Ref. 1. The solid curve is with set 2 except that W is 5.5 MeV. The dotted curve is with set 2 except that W is 12 MeV and r_I is 1.17 fm.

II. EXPERIMENTAL PROCEDURE

The 32 MeV data were measured using the ORNL EN tandem Van de Graaff with the reaction products being detected, at more backward angles, in a position sensitive silicon surface barrier detector (PSD) masked by a 15 angle defining collimator, and at more forward angles, in a dual chamber, position $-\Delta E$, gas proportional counter located at the focal plane of an Enge split-pole magnetic spectrometer. The 15 collimator angle positions were determined optically and their respective solid angles measured using an α source and also by scattering the beam off a gold target. The ^{12}C particle groups were gated by virtue of having the highest energy at a given angle and elastic data were taken simultaneously. The PSD was moved three times with two overlap angles between each position, and three overlap angles were also taken with the magnetic spectrometer measurements. Elastic scattering was measured into a lab angle of 8°, where for absolute normalization purposes the cross section was assumed to be the Rutherford cross reaction

The 68 MeV data employed the ^{11}B beam from the ORNL isochronous cyclotron with the ejectiles being recorded in a similar counter at the focal plane of an Elbek broad range magnetic spectrometer. Elastic scattering data were obtained into a lab angle of 5° for which the cross section is predicted to be within 10% of the Rutherford value. At both energies in the magnetic spectrometer measurements a current integrator and a solid state monitor detector at a fixed angle in the scattering chamber were used to obtain the relative normalization of the data.

III. ANALYSIS

The elastic scattering data at 32 MeV were used to generate two optical model parameter sets, labeled A and B in Table I, employing the search code GENOA.[6] Set A was obtained using the pure volume geometry and set 2 of Ref. 1 as a starting point and letting all six parameters vary to fit the data as seen in Fig. 2. The potential set B was generated by using the shallow *real*, deep imaginary potential ("$E18$") developed by Cramer *et al.*[7] for which the radii and diffuseness were kept fixed, and the two depths were allowed to vary. The parameter set thus generated had an even smaller real to imaginary ratio than did the original $E18$ set. For purposes of comparison the surface transparent potential of Ref. 1 is listed in Table I as C. The bound state geometry for the transfer reaction calculations was the set BS-0 as given by Low and Tamura[8] and also used in Ref. 1. The reaction calculations were carried out using the exact-finite-range DWBA code NICOLE[9] which includes the Coulomb correction terms discussed by DeVries *et al.*[10] as being significant in proton transfer reactions. The transfer reaction data and predicted angular distributions are shown for the two incident energies in Figs. 3, 5, and 7. The 32 MeV data and comparison with the 40 MeV ^{40}Ca(^{13}C, ^{14}N)^{39}K data are discussed first.

In Fig. 3 are shown the theoretical fits to these data obtained by using the pure volume absorption set A in both the entrance and the exit channels. Also shown are curves obtained with the more absorptive set C. The general shapes of the data are fairly well reproduced although the finer details are not. More seriously, the extracted spectro-

TABLE I. Optical model parameters used in analysis of ^{40}Ca(^{11}B, ^{12}C) and (^{13}C, ^{14}N):

$$U(r) = V^C - V(1 + e^X)^{-1} - iW(1 + e^{X'})^{-1} + iW_D 4a_D \frac{d}{dr}(1 + e^{X''})^{-1}$$

$$X = \frac{r - R_R}{a_R}, \quad X' = \frac{r - R_I}{a_I}, \quad X'' = \frac{r - R_D}{a_D}$$

Set	V (MeV)	r_{0R}[a] (fm)	a_R (fm)	W (MeV)	r_{0I}[a] (fm)	a_I (fm)	χ^2/N
A	57.6	1.24	0.53	21.6	1.19	0.60	1.6
B	11.7	1.35	0.618	32.0	1.23	0.552	2.0
C[b]	34.2	1.27	0.55	18.0	1.17	0.05	
				$W_D = 4.5$	$r_{0D} = 1.17$	$a_D = 0.55$	1.3
D[c]	53.6	1.18	0.60	46.6	1.15	0.55	
BS-0[d]	e	1.20	0.65				

[a] $R = r_0(A_T^{1/3} + A_P^{1/3})$ except for BS-0 where $R_R = R_{0R} A_T^{1/3}$.
[b] Reference 1.
[c] Reference 11.
[d] Reference 8.
[e] Depth adjusted to fit the binding energy; a spin-orbit depth of 7 MeV is also present with the same radius and diffuseness.
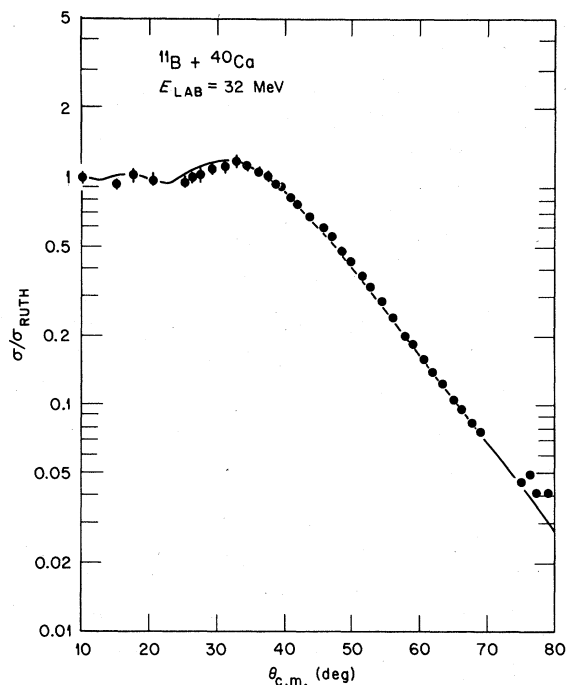
FIG. 2. Elastic scattering data of ^{11}B on ^{40}Ca at 32 MeV. The solid line is the optical model prediction using set A of Table I. Fits using sets B or C would be nearly indistinguishable.
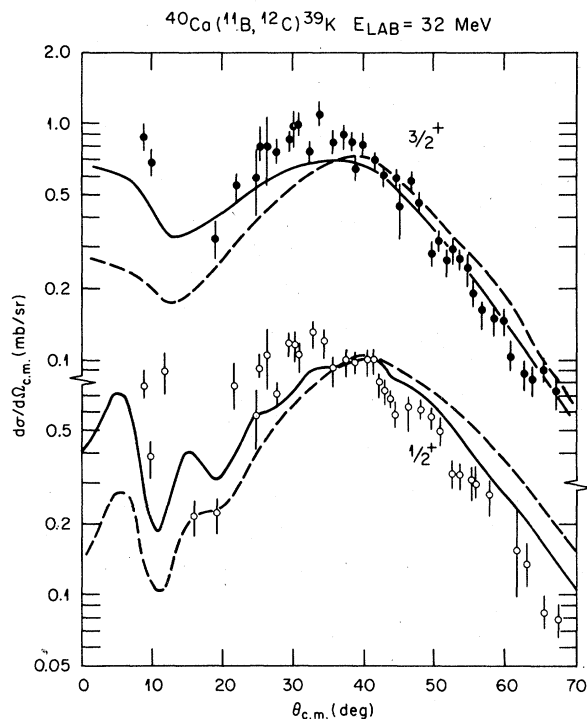

FIG. 3. Angular distributions of the ^{40}Ca(^{11}B, ^{12}C)^{39}K reaction to the ground and first excited states. The solid curves are EFR fits using potential sets A of Table I and the dashed curves are from potential set B.

scopic factors as given in Table II are too high in comparison with the light ion results and also with those of the (^{13}C, ^{14}N) reaction.

The original attempt at fitting the ^{40}Ca(^{13}C, ^{14}N)^{39}K (g.s.) data at 40 MeV was with a very shallow (5.5 MeV) volume absorption term which predicted the solid line curve of Fig. 1. Subsequently this approach was abandoned as it permitted unphysically large contributions from the interior of the nucleus. A less drastic alteration of the imaginary potential ($W = 12$ MeV, $r_1 = 1.17$ fm) significantly improved the quality of the fits (dotted curve of Fig. 1) while preserving more reasonable volume absorption. The potential actually adopted by Baltz et al.[1] for their system, set C of Table I, gives the curve shown in Fig. 4. When this surface transparent potential is used for the ^{40}Ca(^{11}B, ^{12}C)^{39}K reaction, however, the resulting shape is unsatisfactory as shown by the solid curve of Fig. 5. By using potential set A in the entrance channel and set C in the exit channel, one obtains an improvement (dashed curve of Fig. 5), but the fits are still inferior to those shown in Fig. 3. It might be noted that the exit channel ^{12}C + ^{39}K is at nearly the same center of mass energy at 32 MeV as the entrance channel ^{13}C + ^{40}Ca of the ^{40}Ca(^{13}C, ^{14}N) reaction at 40 MeV, so one might have expected similar optical potential descriptions of these channels.

For the 68 MeV data analysis we took the optical potential parameter set developed by Glover et al.,[11] who analyzed ^{12}C + ^{39}K elastic scattering at 54 and 63 MeV. As shown in Fig. 6, the set reproduces our ^{11}B + ^{40}Ca elastic data at 68 MeV. In Fig. 7 are shown the angular distributions predicted for the 68 MeV ^{40}Ca(^{11}B, ^{12}C)^{39}K reactions with the use of the Glover optical potential set in both the entrance and exit channels. The spectro-
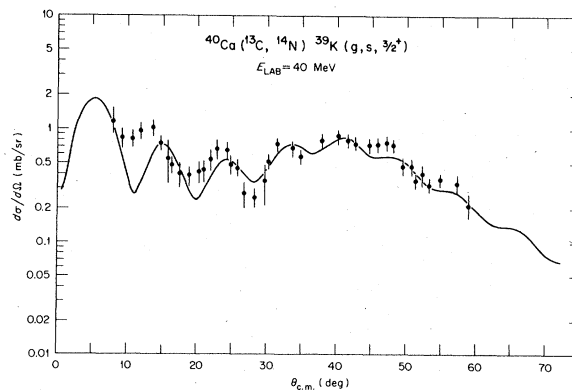

FIG. 4. The same data as in Fig. 1 with the curve being that generated by the surface transparent potential C of Table I. As in Ref. 1 the exit channel imaginary term is *slightly* altered ($W_D = 0.3$ MeV, $r_I = 1.22$ fm).

TABLE II. Spectroscopic factors deduced from light- and heavy-ion induced proton pickup reactions on ^{40}Ca.

^{39}K level E_X(MeV)	mlj	$(d, {}^3\text{He})$ 82 MeV[a]	$({}^{13}\text{C}, {}^{14}\text{N})$ 40 MeV[b]	50 MeV[c]	$({}^{11}\text{B}, {}^{12}\text{C})$[d] 32 MeV	68 MeV
0.0	$1d_{3/2}^{-1}$	3.6	5.0	4.8	8.8 (8.2)[f]	10.1[f]
2.53	$2s_{1/2}^{-1}$	1.1	e	1.7	4.7 (3.7)	3.4
2.82	$1f_{7/2}^{-1}$	0.3	e	e	e	1.8

[a] Reference 17.

[b] Reference 1.

[c] Reference 5.

[d] Present work; assumed 2.85 for the $({}^{11}\text{B}, {}^{12}\text{C})$ spectroscopic factor from Ref. 18. Number in parentheses is obtained using set B of Table I.

[e] Not observed.

[f] See the text for a discussion of the effect of the bound state radius parameter on these values.

scopic factors thus extracted are given in Table II. As at 32 MeV these strengths are larger than obtained in previous measurements. In contrast to the 60 and 68 MeV ^{40}Ca(^{13}C, ^{14}N)^{39}K data,[2] however, the phasing of the predicted shapes is generally in good agreement with the experimental data. Furthermore, if the optical potential which was used to analyze the higher energy (^{13}C, ^{14}N) reactions were used for these (^{11}B, ^{12}C) data, the predictions would not be substantially altered from what is shown here.

IV. DISCUSSION

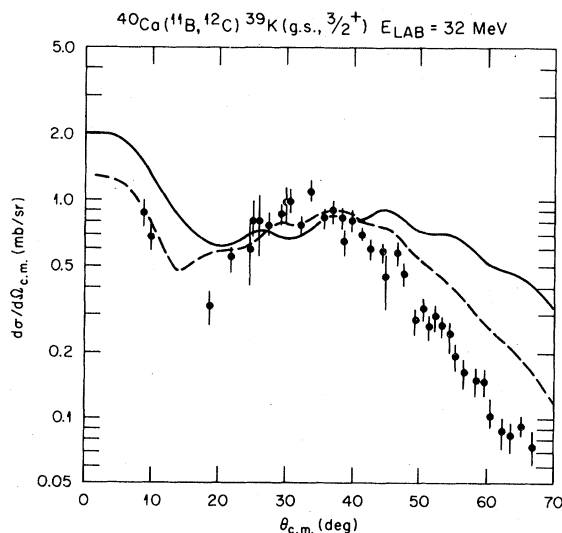There are apparent qualitative differences between the two single-proton pickup reactions (^{13}C, ^{14}N) and (^{11}B, ^{12}C) at both low and high bombarding energies. These differences relate to the success of the DWBA theory in reproducing the shapes and magnitudes of the experimental data. For (^{13}C, ^{14}N) one must resort to a surface transparent potential at 40 MeV which then reproduces the ground state transfer quite well, while at 68 MeV no optical will reproduce the observed shapes but the magnitudes are still correctly given. For (^{11}B, ^{12}C) transfers the shapes are as expected but the theoretical yields are consistently underpredicted.

As has been pointed out previously[12] an important feature affecting the predicted magnitudes is
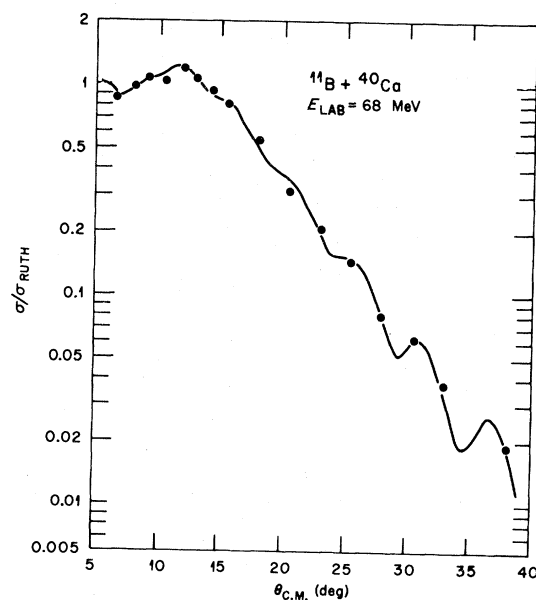

FIG. 5. The ^{40}Ca(^{11}B, ^{12}C) ground state reaction data. The solid curve is calculated with optical potential set C in the exit and entrance channels; the dashed curve with set A in the entrance and set C in the exit channel.

FIG. 6. Elastic scattering data of ^{11}B on ^{40}C at 68 MeV. The curve is an optical model prediction made with the use of set D of Table I.
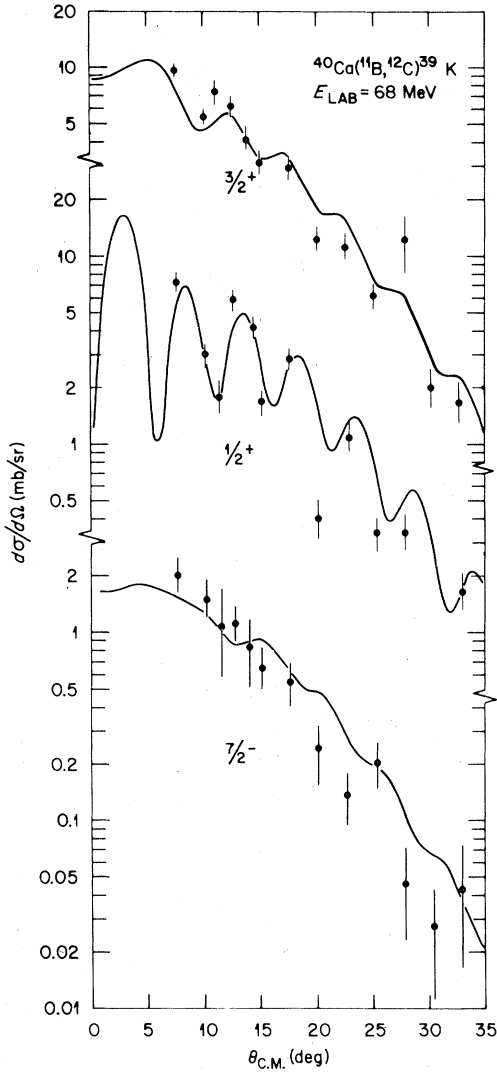
FIG. 7. Transfer reaction data for the ^{40}Ca(^{11}B,^{12}C)^{39}K reaction at an incident energy of 68 MeV. The curve is a fit to the data made with an EFR prediction using optical potential set D.

the choice of the bound state geometry. We have found that by increasing this radius parameter from 1.20 to 1.25 fm, we can systematically *increase* the predicted yields by about 40% and thus decrease the extracted spectroscopic factors by a corresponding amount. In this regard it might be noted that in Ref. 1 the 40 MeV (^{13}C,^{14}N) data were analyzed having the bound state radius parameter as 1.20 fm while for the higher energy (^{13}C,^{14}N) reactions the parameter was taken as 1.25 fm. Hence the lack of consistency in extracted spectroscopic factors between the higher energy (^{13}C,^{14}N) and (^{11}B,^{12}C) experiments is largely, though not completely, due to a different choice of bound state geometry.

Of course, if the 1.25 fm bound state parameter is used to analyze the 40 MeV (^{13}C,^{14}N) data, then the $d_{3/2}$ spectroscopic factor is changed from 5.0 to about 3.6 and then one is faced with a relatively large energy dependent change in the (^{13}C,^{14}N) deduced spectroscopic strengths, such a change not being seen in the (^{11}B,^{12}C) induced reactions. Actually the situation is more complicated because of the 40 MeV (^{13}C,^{14}N) data were analyzed by an approximate finite range program (SRC) (Ref. 13) which does not include the DeVries Coulomb correction terms[10] known now to change the magnitudes of the predicted cross sections by large amounts in charge transfer reactions. These Coulomb correction terms derive from the necessary equivalence of the post and prior forms of the transfer reaction interaction potential ΔV which in the notation of Ref. 10 are given by

$$\Delta V = \Delta V^N + \Delta V^C . \tag{1}$$

The post form is

$$\Delta V^N = V_{bx}^N(\vec{r}_{bx}) + V_{bA}^N(\vec{r}_{bA}) - U_{bB}^N(\vec{r}_b) , \tag{2}$$

$$\Delta V^C = V_{bx}^C(\vec{r}_{bx}) + V_{bA}^C(\vec{r}_{bA}) - U_{bB}^C(\vec{r}_b) , \tag{3}$$

while the prior form is

$$\Delta V^N = V_{xA}^N(\vec{r}_{xA}) + V_{bA}^N(\vec{r}_{bA}) - U_{aA}^N(\vec{r}_a) , \tag{4}$$

$$\Delta V^C = V_{xA}^C(\vec{r}_{xA}) + V_{bA}^C(\vec{r}_{bA}) - U_{aA}^C(\vec{r}_a) . \tag{5}$$

The reaction notation is $A(a,b)B$ with $a = b + x$, $B = A + x$, and x being the transferred particle. The superscript C refers to the Coulomb part and the superscript N to the nuclear part of the interaction, and U is the optical potential in either the exit or the entrance channel. The Coulomb correction terms are given by (3) or (5) and can be included exactly while it is assumed that the exact (and unknown) nuclear core-core term V_{bA}^N and the nuclear part of the optical potential U^N cancel out. Since these correction terms are important[10] near the Coulomb barrier, we have undertaken the complete post-prior comparison of the 32 MeV (^{11}B,^{12}C) and the 40 MeV (^{13}C,^{14}N) reactions. The results of that analysis are presented in Table III.

As expected the inclusion of the ΔV^C terms has a significant effect in the size of the predicted cross sections, more so in the prior than in the post calculations in line with the results of DeVries *et al.*[10] It is seen from Table III that in the (^{11}B,^{12}C) reactions there is little remaining post-prior discrepancy with the Coulomb correction terms included. Somewhat unexpectedly, however, there remains a substantially large discrepancy between the post and prior results for the (^{13}C,^{14}N) reactions, most especially for the $2s_{1/2}$ state which was not recorded experimentally. We have established that these discrepancies are related to the choice

TABLE III. Post-prior comparisons of (^{11}B, ^{12}C) and (^{13}C, ^{14}N) reactions on ^{40}Ca.

Reaction	Final state	ΔV^C with or without	Post or prior	$\sigma(\theta_p)$ [a]	σ_{total} [a]	Potential [b] set
(^{11}B, ^{12}C)	$\frac{3}{2}^+$	With	Post	0.253	0.533	A
			Prior	0.259	0.543	A
		Without	Post	0.300	0.640	A
			Prior	0.390	0.800	A
	$\frac{1}{2}^+$	With	Post	0.678	1.59	A
			Prior	0.700	1.61	A
		Without	Post	0.822	1.86	A
			Prior	1.01	2.23	A
(^{13}C, ^{14}N)	$\frac{3}{2}^+$	With	Post	0.518	1.13	C [c]
			Prior	0.691	1.32	C
		Without	Post	0.682	1.44	C
			Prior	1.05	1.94	C
	$\frac{1}{2}^+$	With	Post	0.699	1.59	C
			Prior	1.17	2.67	C
		Without	Post	0.808	2.13	C
			Prior	1.54	3.43	C
	$\frac{3}{2}^+$	With	Post	0.371	0.751	A
			Prior	0.418	0.799	A
(^{13}C, ^{14}N)	$\frac{1}{2}^+$	With	Post	0.393	1.23	A
			Prior	0.456	1.27	A

[a] Cross section in arbitrary units, with θ_p for (^{11}B, ^{12}C) at 34° and θ_p for (^{13}C, ^{14}N) at 40°; σ_{total} is integrated differential cross section.
[b] Potential set as given in Table I.
[c] As in Ref. 1 the ^{14}N + ^{39}K optical potential was modified from set C given in Table I.

of the optical potential by repeating the (^{13}C, ^{14}N) calculations with the ^{11}B optical potential set A and the results of that analysis are also given in Table III. With the use of this optical potential set the post-prior discrepancy for (^{13}C, ^{14}N) is mostly eliminated. An interpretation of these results is that the surface transparent optical potential is not a good representation of the exact core-core interaction V_{bA}^N at least insofar as the evaluation of the transfer reaction amplitude is concerned. Such an interpretation is counter to the analysis presented in Ref. 1. On the other hand, the use of the standard volume absorption set A, while it does not suffer a major post-prior discrepancy, will not reproduce the angular distribution of (^{13}C, ^{14}N) giving a shape like the dashed line in Fig. 1. The use of set A would also give a much larger spectroscopic factor than set C. We thus conclude that the ^{40}Ca(^{13}C, ^{14}N)^{39}K reaction at 40 MeV is not well understood and these data may well be related to the anomalous behavior of this reaction at higher energies.

Regarding the analysis of the 68 MeV (^{13}C, ^{14}N) angular distribution data, it has been suggested[14] that the inclusion of a spin orbit term in the optical potential would substantially improve the theoretical fit. That analysis, however, was based on a no-recoil approximation to the transition amplitude, an approximation which is less trustworthy for $j_<$ to $j_<$ (Ref. 15) transfers as is the case here. In Fig. 8 we show a comparison of the no-recoil
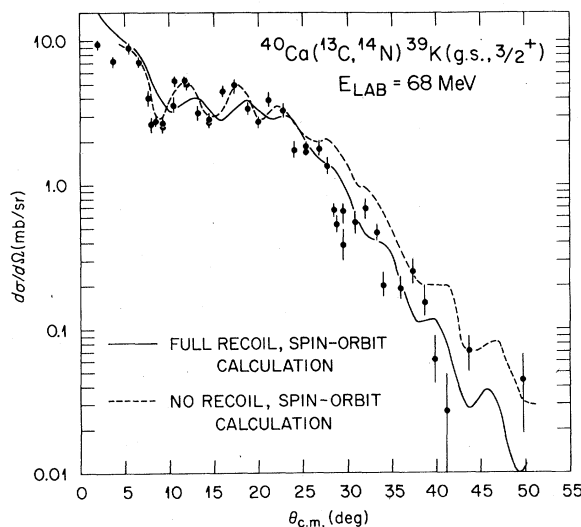

FIG. 8. The ^{40}Ca(^{13}C, ^{14}N)^{39}K (g.s.) transfer reaction data are from Ref. 2. The dashed curve is a no-recoil finite range calculation including a spin-orbit coupling potential obtained by Bayman *et al.* (Ref. 14). The solid curve is the same calculation except that it treats recoil exactly.

and full-recoil predictions using the same optical potentials including spin orbit. The exact calculation is still out of phase with the data and attempts to bring it in phase with the data by changing the value of the spin orbit depth were unsuccessful. Of course, another choice of a spin-orbit optical potential may be successful. This comparison merely shows that any such conclusion must be based on a full recoil calculation.

V. SUMMARY

The ^{40}Ca(^{13}C, ^{14}N)^{39}K and ^{40}Ca(^{11}B, ^{12}C) reactions have been compared at similar bombarding energies. The (^{11}B, ^{12}C) reactions have angular distributions which are reasonably well predicted by the DWBA theory but have yields which can be accounted for only by choosing a larger bound states radius parameter than has been customary. The spectroscopic factors thus extracted are consistent between 32 and 68 MeV incident energy. The surface transparent potential which was used in reproducing the 40 MeV (^{13}C, ^{14}N) reaction is unsatisfactory for (^{11}B, ^{12}C) although the kinetic energies are comparable between these two systems. A closer analysis of the lower energy (^{13}C, ^{14}N) reaction with the surface transparent potential reveals a serious post-prior discrepancy not present when standard volume absorption is used. Hence, the ^{40}Ca(^{13}C, ^{14}N) reaction data appear to be anomalous in shape at both low and high bombarding energies. A coupled channels approach has been suggested[16] for the explanation of the 68 MeV data, and it would be interesting to see if such a calculation were also effective at 40 MeV incident energy with a standard optical potential.

[1] A. J. Baltz, P. D. Bond, J. D. Garrett, and S. Kahana, Phys. Rev. C 12, 136 (1975); P. D. Bond, J. D. Garrett, S. Kahana, M. J. Levine, and A. Z. Schwarzchild, in *Proceedings of the International Conference on Reactions Between Complex Nuclei, Nashville, Tennessee, 1974*, edited by R. L. Robinson, F. K. McGowan, J. B. Ball, and J. H. Hamilton (North-Holland, Amsterdam/American Elsevier, New York, 1974), Vol. I, p. 54.

[2] P. D. Bond, C. Chasman, J. D. Garrett, C. K. Gelbke, O. Hansen, M. J. Levine, A. Z. Schwarzchild, and C. E. Thorn, Phys. Rev. Lett. 35, 300 (1976).

[3] K.-I. Kubo, K. G. Nair, and K. Nagatani, Phys. Rev. Lett. 37, 222 (1976).

[4] W. Treu, C. W. Towsley, K. G. Nair, and H. Voit, Phys. Rev. C 19, 96 (1979).

[5] P. D. Bond, M. J. LeVine, D. J. Pisano, C. E. Thorn, and L. L. Lee, Jr., Phys. Rev. C 19, 2160 (1979).

[6] F. Perey (unpublished).

[7] J. G. Cramer, R. M. DeVries, D. A. Goldberg, M. S. Zisman, and C. F. Maguire, Phys. Rev. C 14, 2158 (1976).

[8] K. S. Low and T. Tamura, Phys. Rev. C 11, 789 (1975).

[9] C. F. Maguire, Phys. Rev. C 20, 1037 (1979).

[10] R. M. DeVries, G. R. Satchler, and J. G. Cramer, Phys. Rev. Lett. 1377 (1974).

[11] C. W. Glover, K. W. Kemper, L. A. Parlso, F. Petrovich, and D. P. Stanley (unpublished).

[12] S. C. Pieper et al., Phys. Rev. C 18, 180 (1978).

[13] A. J. Baltz and S. Kahana, Phys. Rev. C 9, 2243 (1974).

[14] B. F. Bayman, A. Dudek-Ellis and P. J. Elles, Nucl. Phys. A301, 141 (1978).

[15] T. Tamura, Phys. Rep. 14, 59 (1974).

[16] S. Kubono, S. J. Tripp, D. Dehnhard, T. Udagawa, and T. Tamura, Phys. Rev. C 18, 1929 (1978).

[17] H. Doubre, D. Royer, Mardite L. Bimbot, N. Frascaria, J. P. Carron, and M. Riou, Phys. Lett. 29B, 355 (1969).

[18] S. Cohen and D. Kurath, Nucl. Phys. A101, 1 (1967).